ACS APPLIED ENERGY MATERIALS

www.acsaem.org Letter

Promoting Methane Hydrate Formation for Natural Gas Storage over Chabazite Zeolites

Shurraya Denning, Ahmad AA Majid, James M. Crawford, Moises A. Carreon,* and Carolyn A. Koh*

Cite This: ACS Appl. Energy Mater. 2021, 4, 13420−13424 Read Online

ACCESS | Metrics & More | Article Recommendations | Supporting Information

ABSTRACT: Gas hydrates are a promising methane storage method. This study investigates the potential for zeolites to overcome hydrate formation limitations. The chabazite zeolites SSZ-13 and SAPO-34 increased water-to-hydrate conversion from 5.8 ± 1.4% to 91.3 ± 0.5% and 38.4 ± 1.5%, respectively, due to the high surface area of the zeolites enlarging the gas-to-water contact area. SSZ-13 promoted on average 2.6 times more hydrate growth than SAPO-34 due to SSZ-13's more hydrophobic nature resulting in higher methane adsorption (can be consumed in hydrate formation) and lower electrostaticity (does not restrict water activity/orientation). Overall, SSZ-13 maintains its structural integrity and exhibits reproducible hydrate formation promotion results.

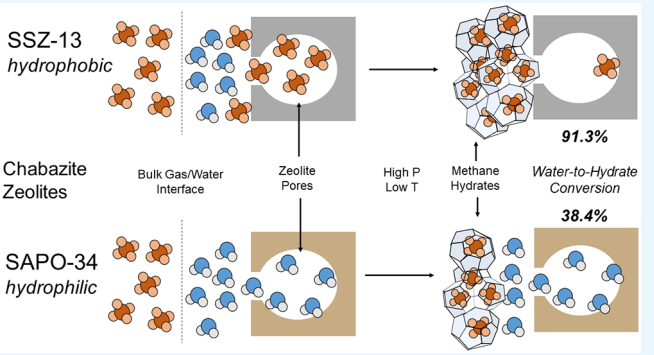

KEYWORDS: *gas hydrates, chabazite zeolites, gas storage, natural gas, hydrophobicity, hydrate promoter*

Globally, the increasing rate of energy usage relies upon natural gas to meet the demand. Natural gas, consisting primarily of methane, is sought after as it is a relatively clean energy source and occurs abundantly.[1,2] A limitation of natural gas stems from methane's low density resulting in low energy content per volume, making storage and transportation expensive.[1]

An effective approach for gas storage is the use of gas hydrates. Gas hydrates consist of water molecules that form hydrogen bonds to encage a guest molecule, such as methane.[3] Pure methane hydrates crystallize as structure I, illustrated in Figure 1(a).[4]

Gas hydrates typically form under high pressure and low temperature conditions, depending upon the guest molecule present.[3] Some attractive aspects of gas hydrates are they have high methane storage capacities (~160 m^3 of methane fits in 1 m^3 of hydrate at STP) and they are benign environmentally (hydrates consist only of water and gas).[3]

From the transportation viewpoint, gas hydrates are appealing due to the "self-preservation" phenomenon, which prolongs hydrate stability at modest temperatures.[6] This phenomenon is believed to result from a shielding ice layer on the surface of the gas hydrate, which prevents the escape of host gases, thus maintaining stability at ambient pressure and below the freezing temperature of ice.[3,6] One study preserved methane hydrates with THF as an additive at ambient pressure and −2 °C for 2 years.[7]

Although alluring, high water-to-hydrate conversion can be difficult to achieve in a static, pure methane and water system.[8] Low gas-to-water contact area inhibits hydrate growth, as hydrates start forming at this interface thus limiting gas diffusion to the now trapped water phase.[8,9] Local heat of formation can

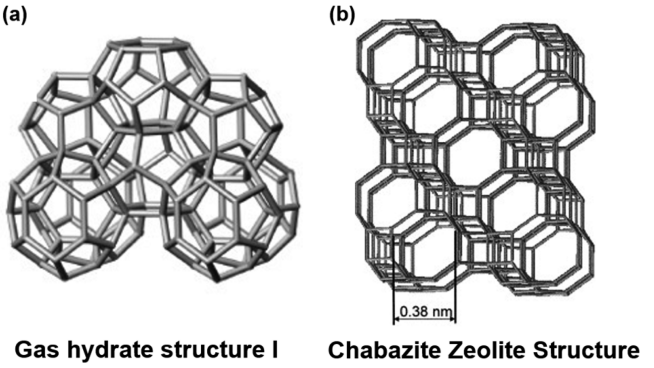

Figure 1. Representative illustrations of (a) gas hydrate structure I with unit cell diameter 1.2 nm[4] and (b) the chabazite zeolite structure with a limiting pore window of 0.38 nm.[5] Not to scale. Reproduced with permission from ref 4. Copyright 2007 John Wiley and Sons. Reproduced with permission from ref 5. Copyright 2004 Elsevier.

Received: September 17, 2021
Accepted: December 7, 2021
Published: December 15, 2021

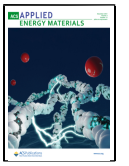

slow hydrate growth if not removed, and impeded water ordering may prevent hydrate cages from forming.[10,11]

Several approaches have been proposed to overcome these barriers, such as adding chemical additives,[12,13] modifying apparatus design,[14,15] and using porous materials. In particular, porous materials provide multiple advantages for hydrate promotion: large surface area (e.g., increases gas-to-water contact area)[9] and good surface chemistry (e.g., removes local heat of formation,[11] positively affects water ordering,[10] or adsorbs methane[16]). In addition, pore size and channel shape/topology can influence hydrate promotion.[17]

A wide assortment of porous materials are undergoing research, such as organic (e.g., activated carbon[18]), hybrid organic−inorganic (e.g., metal organic frameworks[19,20]), and inorganic (e.g., zeolites[8,13,15,21,22]) among others. Zeolites are suitable porous materials due to their high mechanical and thermal stability, large surface areas, and tunable surface chemistry. As far as the authors are aware, few zeolites have been reported as methane hydrate promoters: RHO,[8] 13A,[21] 13X,[21,22] 3A,[15] and 5A.[13,21]

Two small pore zeolites suitable as promoters for methane hydrate formation are SAPO-34 and SSZ-13. These zeolites crystallize in the same chabazite topology, illustrated in Figure 1(b); thus, both have limiting pore apertures of 3.8 Å, an internal pore diameter of ∼7.4 Å, and surface areas in the ∼450−550 m^2/g range.[5,23]

These zeolites differ in composition and surface chemistry: SAPO-34 contains silica, alumina, and phosphate, leading to a relatively hydrophilic surface,[24] whereas SSZ-13 only contains silica and alumina, resulting in a more hydrophobic surface.[25] Hydrophobicity influences methane hydrate formation due to its effect on the tetrahedral water ordering needed for hydrate formation.[10,26] A comparison of SAPO-34 and SSZ-13 would provide insight into the effect of hydrophobicity in methane hydrate formation without variance from pore structure differences.

In this study, we determined the performance of SAPO-34 and SSZ-13 in promoting methane hydrate formation. Detailed synthesis instructions along with equipment and procedures for zeolite characterization and observing hydrate formation are given in the Supporting Information. Without any zeolite present in the HP-DSC, only 5.8 ± 1.4% of the water was converted into hydrate. SSZ-13, the more hydrophobic zeolite due to the high Si/Al ratio in its framework, converted as high as 91.3 ± 0.5% of the water to hydrate, whereas SAPO-34, the more hydrophilic of the two zeolites due to its low Si/Al, only converted as high as 38.4 ± 1.5%. Thus, SSZ-13 outperformed SAPO-34 as a promoter for improving water-to-hydrate conversion, evident in Figure 2.

The amount of hydrate converted for both zeolites depended upon the mass ratio of water to zeolite (R_w). The values reported in Figure 2 are summarized in Tables S1 and S2 for SAPO-34 and SSZ-13, respectively. The warming HP-DSC profiles corresponding to each R_w are given, respectively, in Figures S2 and S3. Both zeolites promote hydrate growth at their respective optimal mass ratios as a result of their large surface areas leading to an enhanced gas-to-water contact area. Notably, no hydrates should form inside of the pores as the pores of these zeolites (0.74 nm in diameter)[5] are too small for the methane hydrate structure I unit cell (1.2 nm).[3]

The discrepancy in water-to-hydrate conversion between SSZ-13 and SAPO-34 is associated with the zeolite's hydrophobicity, which affects the wetting of the zeolite particles. The

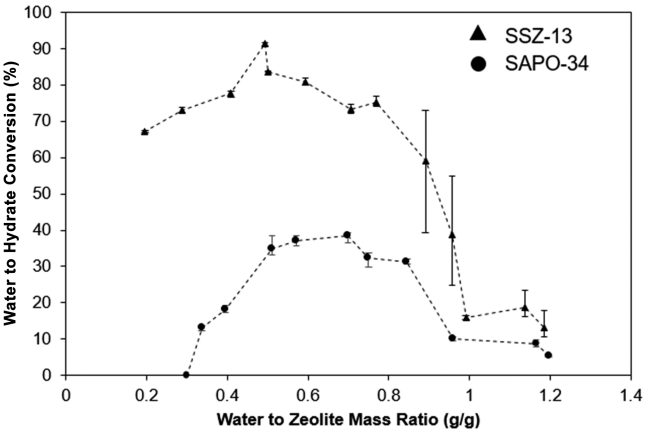

Figure 2. Water-to-hydrate conversion as a function of the water-to-zeolite mass ratios for SSZ-13 and SAPO-34. Conversion is calculated from scanning experiments in the HP-DSC conducted at 8.0 MPa.

measured amount of water adsorbed by SSZ-13 (7 mmol/g) is significantly less than that of SAPO-34 (16 mmol/g), indicating that SSZ-13 is more hydrophobic than SAPO-34. The effect of hydrophilicity arises especially in the water to zeolite mass ratio (R_w) of 0.3, denoted as a partially saturated bed. At this R_w, SSZ-13 converted 73.0 ± 0.8% of water into hydrate and does not form any ice. This observation results from the hydrophobicity of SSZ-13 leading to high adsorption of methane in its pores and on the external surface of the particles, which can then be consumed in hydrate formation, as depicted in Figure 3(a).[26] The large surface area of SSZ-13 results in a thin water layer around the particles, which in principle would promote a thin layer of hydrate formation and thus explain the lack of ice formation.

In comparison, in a partially saturated bed of SAPO-34 with an R_w = 0.3, no hydrate or ice formation was observed. Therefore, all of the water in the HP-DSC system fills the SAPO-34 pores, as illustrated in Figure 3(b), where the zeolite particles are tinted blue.[24] The lack of water outside of the SAPO-34 particles results in no formation of hydrate or ice.

The difference in optimal R_w for the two zeolites also supports the hypothesis that hydrophobicity plays a primary role in how a zeolite can promote water-to-hydrate conversion. As evident in Figure 2, the optimal R_w for SSZ-13 (R_w = 0.49) is lower than the optimum for SAPO-34 (R_w = 0.7). The system with SAPO-34 requires more water to reach its optimal ratio due to the hydrophilicity preferentially filling the pores of SAPO-34 with water. This trapped water cannot convert to hydrate as the pores of SAPO-34 are too small. Thus, a higher ratio of water to zeolite is necessary to create the desirable thin layer of water around the SAPO-34 particles, as the thin layer maximizes the gas-to-water contact area. The relative hydrophobicity of SSZ-13 does not preferentially fill its pores with water; consequently, the desirable thin layer of water is reached at a lower water to zeolite ratio.

In the oversaturated saturated scenario (R_w > 1.2), SSZ-13 converts more than twice as much hydrate as SAPO-34 (13.1% versus 5.3%, respectively). This difference could result from the adsorbed methane on the surface of SSZ-13 (both inside the pores and on the external surface), creating a thin layer of methane or methane bubbles on the external surface of the particle, illustrated in Figure 3(c).[16] The adsorbed methane may be consumed in methane hydrate formation, resulting in an overall increased gas-to-water contact area relative to a system

https://doi.org/10.1021/acsaem.1c02902
ACS Appl. Energy Mater. 2021, 4, 13420−13424

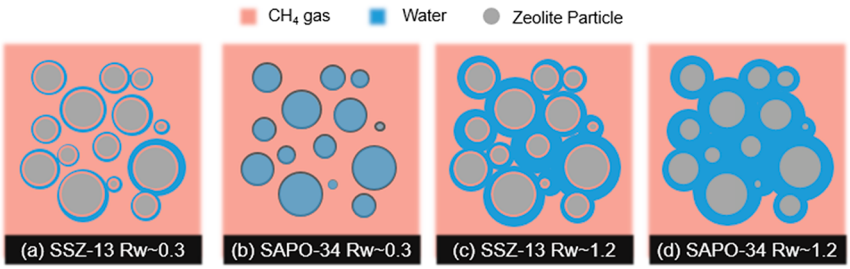

Figure 3. Illustration of packing in (a) a partially saturated SSZ-13 bed, (b) a partially saturated SAPO-34 bed, (c) an oversaturated SSZ-13 bed, and (d) an oversaturated SAPO-34 bed. Pink represents methane gas, blue represents water, and gray represents zeolite particles. Reproduced with permission from ref 26. Copyright 2020 American Chemical Society.

without any hydrates.[16] Despite SSZ-13 and SAPO-34 adsorbing a similar amount of methane (0.53 mmol/g versus 0.52 mmol/g at 1 bar and 20 °C, respectively), the competitive adsorption between water and methane dominates how much methane is adsorbed in the hydrate formation conditions. The methane adsorption isotherms are shown in Figure S4. The ratio of water to methane adsorbed for SAPO-34 is 31.5, which is 2.4 times more than SSZ-13 at 13.1. Note that these ratios are similar to a study in the literature on the adsorption of methane and water on these zeolites.[27] Similar to the low R_w scenario with SAPO-34, at the high R_w the water blocks the pores. A study on how humidity affects SAPO-34 found that the adsorbed water completely blocked the pores, preventing the permeation of methane through the material.[24] These observations aid in explaining why at $R_w \sim 1.2$, the conversion in a system with SAPO-34 (5.3 ± 0.3%) is nearly the same as a system without any zeolite (5.8 ± 1.4%). The lack of readily available adsorbed methane on SAPO-34 is illustrated in Figure 3(d). The competitive adsorption affects the performance of the zeolites at all other water to zeolite mass ratios, with conversions averaging 2.6 times more for SSZ-13 compared to SAPO-34.

Interestingly, both zeolites showed a similar trend with regard to their effect on the hydrate dissociation temperature. As the amount of water in the system decreased (i.e., zeolite to water mass ratio decreased), the dissociation temperature decreased, as shown in Figure 4.

Although the difference in dissociation temperature (system without zeolite versus system with zeolite) is nearly commensurate with the precision of the HP-DSC (±0.5 °C), the trend is distinct for each zeolite with small deviations.

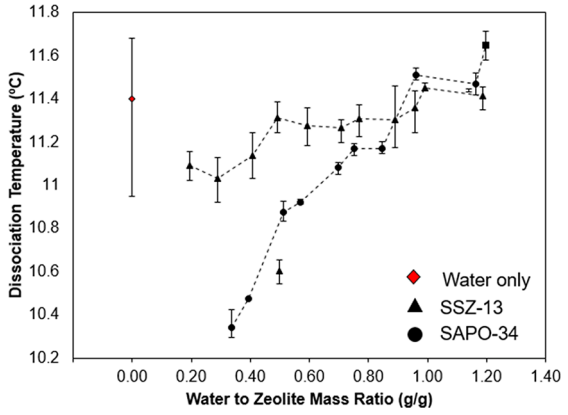

Figure 4. Hydrate dissociation temperature for bulk water (red diamond) and for different water to zeolite mass ratios for SSZ-13 (black triangle) and SAPO-34 (black circles).

Studies in the literature found that a decrease in hydrate dissociation temperature correlates to thermodynamic inhibition, which can be caused by hydrates forming in a confined space, such as the interparticle spacing, restricting the water activity and in consequence shifting the phase envelope.[17,28] To reiterate, the pores of both zeolites in this study (~0.74 nm, shown in nitrogen adsorption isotherms at 77 K in Figure S5) are too small for hydrate formation (structure I unit cell size 1.2 nm) to take place within the pores; thus, the formation is most likely taking place in the interparticle spacing.

The effect of zeolite hydrophobicity on the wetting of the zeolite particles may contribute to SAPO-34 depressing the dissociation temperature at lower water content more than SSZ-13. The hydrophilicity of SAPO-34 may hold water in interstitial and interparticle spaces better than the hydrophobic SSZ-13.[26] Although at a lesser extent, the system with SSZ-13 also experiences a decreasing trend in dissociation temperature, as SSZ-13 is not completely hydrophobic due to the presence of Al in the structure (Si/Al molar ratio is 20).

Furthermore, the higher electrostatic interactions of SAPO-34 due to the high Al content and the presence of phosphorus in the structure can reduce the water activity coefficient, which can cause thermodynamic inhibition.[3] In SSZ-13, the high content of Si leads to low electrostatic interactions, yet the presence of the small amount of Al can explain why a small decrease is still observed. Thus, the reactivity and hydrophilicity of SAPO-34 may be the dominating factors leading to the reduced hydrate dissociation temperatures.

To ensure that a difference in zeolite particle size was not a contributing factor in hydrate formation and dissociation, SEM images of SSZ-13 and SAPO-34 were taken and the particles measured, as shown in Figure 5(left).

The overall particle size distributions of SSZ-13 (0.51−3.76 μm) and SAPO-34 (0.38−3.64 μm) were similar. Therefore, it is unlikely that the size of the particles influenced the depressed dissociation temperature.

The XRD patterns, given in Figure 5(right), show that the synthesized zeolites match the simulated chabazite zeolite pattern well. Although both pre and post HP-DSC zeolite patterns exhibit no observable change in peak location, the intensity ratios of the peaks change slightly for both zeolites. The (100)/(20−1) plane intensity ratio decreased by a factor of 1.45 for SAPO-34 and 0.48 for SSZ-13. This change in preferential plane exposure may result from water influencing the crystallinity of the samples. As expected, SAPO-34 exhibits a larger change, as one study in the literature found that in a humid environment, SAPO-34 was prone to degrade to a greater extent over time.[24] The higher stability of SSZ-13 also stems from its higher Si/Al ratio as compared to SAPO-34 with a low Si/Al

https://doi.org/10.1021/acsaem.1c02902
ACS Appl. Energy Mater. 2021, 4, 13420−13424

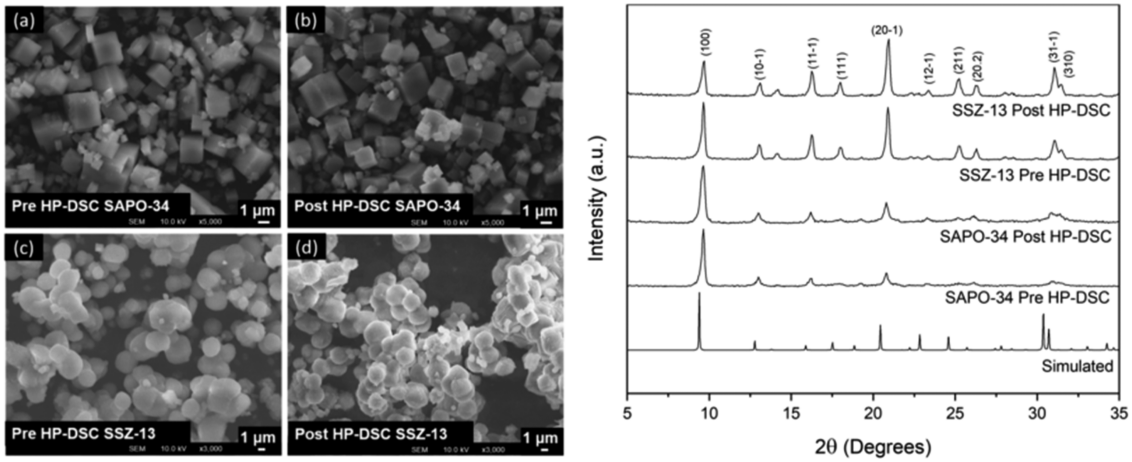

Figure 5. (Left) SEM images of SAPO-34 (a) pre HP-DSC and (b) post HP-DSC, and SSZ-13 (c) pre HP-DSC and (d) post HP-DSC. (Right) XRD patterns for simulated chabazite and for measured SAPO-34 and SSZ-13 pre and post HP-DSC.

ratio, as one study found that the stability of these zeolites in humid environments increased with increasing Si/Al ratios.[29]

Overall, both SAPO-34 and SSZ-13 maintain their morphology and crystallinity after three consecutive cycles of hydrate formation and dissociation, as evident in the SEM images and XRD patterns given in Figure 5. This structural integrity indicates that the zeolites are recyclable, lending to the materials having a long lifecycle as hydrate promoters.

The previous work completed by our group using the metal organic frameworks HKUST-1, ZIF-8, and ZIF-67 as methane hydrate promoters exhibited similar high water-to-hydrate conversion results as SSZ-13.[19,20] The most advantageous aspect of using zeolites instead of metal organic frameworks is that the process for producing zeolites is already well established. Zeolites are composed of nonprecious metals/metalloids (i.e., aluminum and silica) as compared to the metal organic frameworks which use copper (HKUST-1), zinc (ZIF-8), or cobalt (ZIF-67). Therefore, SSZ-13 is highly desirable as it provides a more cost-effective approach while also producing the same high hydrate yield.

In summary, we demonstrated how the chabazite zeolites SSZ-13 and SAPO-34 promoted methane hydrate growth by increasing the water-to-hydrate conversion. The more hydrophobic zeolite, SSZ-13, on average over a range of different water to zeolite mass ratios converted 2.6 times more water into hydrate than SAPO-34. The better performance of SSZ-13 as a hydrate promoter is associated with its hydrophobic nature aiding in correctly orienting water molecules for hydrate formation and its lower water-to-methane adsorption ratio (13.1), as compared to SAPO-34 (31.5), thus providing an additional gas-to-water contact area at the surface of the material. The low Si/Al ratio in SAPO-34 (Si/Al of 0.6) resulted in a more electrostatic structure than SSZ-13 (Si/Al of 20), which ended up thermodynamically inhibiting the hydrates in a system with lower water content. The mechanical stability and preservation of crystal integrity after multiple cycles of hydrate formation and dissociation, combined with the induced high water-to-hydrate conversion, suggest that SSZ-13 is a highly appealing candidate as a methane hydrate promoter for natural gas storage.

■ ASSOCIATED CONTENT

Supporting Information

The Supporting Information is available free of charge at https://pubs.acs.org/doi/10.1021/acsaem.1c02902.

Detailed procedure of the synthesis of the zeolites SAPO-34 and SSZ-13. Description of the methods used to characterize the zeolites. Procedures, calculations, and equipment description for observing and quantifying hydrate formation behavior. Warming profiles for HP-DSC experiments and tabulated conversion and hydrate dissociation temperature. Isotherms for methane at 293 K and nitrogen at 77K (PDF)

■ AUTHOR INFORMATION

Corresponding Authors

Moises A. Carreon − *Chemical and Biological Engineering Department, Colorado School of Mines, Golden, Colorado 80401, United States;* orcid.org/0000-0001-6391-2478; Email: mcarreon@mines.edu

Carolyn A. Koh − *Chemical and Biological Engineering Department, Colorado School of Mines, Golden, Colorado 80401, United States;* orcid.org/0000-0003-3452-4032; Email: ckoh@mines.edu

Authors

Shurraya Denning − *Chemical and Biological Engineering Department, Colorado School of Mines, Golden, Colorado 80401, United States*

Ahmad AA Majid − *Chemical and Biological Engineering Department, Colorado School of Mines, Golden, Colorado 80401, United States*

James M. Crawford − *Chemical and Biological Engineering Department, Colorado School of Mines, Golden, Colorado 80401, United States*

Complete contact information is available at: https://pubs.acs.org/10.1021/acsaem.1c02902

Notes

The authors declare no competing financial interest.

https://doi.org/10.1021/acsaem.1c02902
ACS Appl. Energy Mater. 2021, 4, 13420−13424

■ ACKNOWLEDGMENTS

The financial support provided by the National Science Foundation (CBET award # 1835924) is gratefully acknowledged.

■ REFERENCES

(1) Demirbas, A. The Importance of Natural Gas as a World Fuel. *Energy Sources, Part B* **2006**, *1* (4), 413−420.
(2) Collett, T.; Bahk, J. J.; Baker, R.; Boswell, R.; Divins, D.; Frye, M.; Goldberg, D.; Husebø, J.; Koh, C.; Malone, M.; Morell, M.; Myers, G.; Shipp, C.; Torres, M. Methane Hydrates in Nature-Current Knowledge and Challenges. *J. Chem. Eng. Data* **2015**, *60* (2), 319−329.
(3) Sloan, E. D.; Koh, C. A. *Clathrate Hydrates of Natural Gases*, 3rd ed.; CRC Press: Boca Raton, FL, 2008.
(4) Koh, C. A.; Sloan, E. D. Natural Gas Hydrates: Recent Advances and Challenges in Energy and Environmental Applications. *AIChE J.* **2007**, *53* (7), 1636−1643.
(5) Li, S.; Falconer, J. L.; Noble, R. D. SAPO-34 Membranes for CO2/CH4 Separation. *J. Membr. Sci.* **2004**, *241* (1), 121−135.
(6) Gudmundsson, J.; Borrehaug, A. Frozen Hydrate for Transport of Natural Gas. *International Conference on Natural Gas Hydrates*; Toulouse, 1996; pp 415−422.
(7) Bhattacharjee, G.; Veluswamy, H. P.; Kumar, A.; Linga, P. Stability Analysis of Methane Hydrates for Gas Storage Application. *Chem. Eng. J.* **2021**, *415*, 128927.
(8) Andres-Garcia, E.; Dikhtiarenko, A.; Fauth, F.; Silvestre-Albero, J.; Ramos-Fernández, E. V.; Gascon, J.; Corma, A.; Kapteijn, F. Methane Hydrates: Nucleation in Microporous Materials. *Chem. Eng. J.* **2019**, *360*, 569−576.
(9) Cuadrado-Collados, C.; Mouchaham, G.; Daemen, L.; Cheng, Y.; Ramirez-Cuesta, A.; Aggarwal, H.; Missyul, A.; Eddaoudi, M.; Belmabkhout, Y.; Silvestre-Albero, J. Quest for an Optimal Methane Hydrate Formation in the Pores of Hydrolytically Stable Metal-Organic Frameworks. *J. Am. Chem. Soc.* **2020**, *142* (31), 13391−13397.
(10) Nguyen, N. N.; Nguyen, A. V. Hydrophobic Effect on Gas Hydrate Formation in the Presence of Additives. *Energy Fuels* **2017**, *31* (10), 10311−10323.
(11) Ling, Z.; Zhou, H.; Dong, H.; Shi, C.; Zhao, J.; Liu, H.; Song, Y. MXene (Ti3C2Tx) as a Promising Substrate for Methane Storage via Enhanced Gas Hydrate Formation. *J. Phys. Chem. Lett.* **2021**, *12*, 6622−6627.
(12) Gupta, P.; Chandrasekharan Nair, V.; Sangwai, J. S. Phase Equilibrium of Methane Hydrate in the Presence of Aqueous Solutions of Quaternary Ammonium Salts. *J. Chem. Eng. Data* **2018**, *63* (7), 2410−2419.
(13) Zhao, Y.; Zhao, J.; Liang, W.; Gao, Q.; Yang, D. Semi-Clathrate Hydrate Process of Methane in Porous Media-Microporous Materials of 5A-Type Zeolites. *Fuel* **2018**, *220*, 185−191.
(14) Rossi, F.; Filipponi, M.; Castellani, B. Investigation on a Novel Reactor for Gas Hydrate Production. *Appl. Energy* **2012**, *99*, 167−172.
(15) Zang, X.; Du, J.; Liang, D.; Fan, S.; Tang, C. Influence of A-Type Zeolite on Methane Hydrate Formation. *Chin. J. Chem. Eng.* **2009**, *17* (5), 854−859.
(16) Guo, Y.; Xiao, W.; Pu, W.; Hu, J.; Zhao, J.; Zhang, L. CH4 Nanobubbles on the Hydrophobic Solid-Water Interface Serving as the Nucleation Sites of Methane Hydrate. *Langmuir* **2018**, *34* (34), 10181−10186.
(17) Borchardt, L.; Casco, M. E.; Silvestre-Albero, J. Methane Hydrate in Confined Spaces: An Alternative Storage System. *ChemPhysChem* **2018**, *19* (11), 1298−1314.
(18) Cuadrado-Collados, C.; Majid, A. A. A.; Martínez-Escandell, M.; Daemen, L. L.; Missyul, A.; Koh, C.; Silvestre-Albero, J. Freezing/Melting of Water in the Confined Nanospace of Carbon Materials: Effect of an External Stimulus. *Carbon* **2020**, *158*, 346−355.
(19) Denning, S.; Majid, A. A. A.; Lucero, J. M.; Crawford, J. M.; Carreon, M. A.; Koh, C. A. Methane Hydrate Growth Promoted by Microporous Zeolitic Imidazolate Frameworks ZIF-8 and ZIF-67 for Enhanced Methane Storage. *ACS Sustainable Chem. Eng.* **2021**, *9* (27), 9001−9010.
(20) Denning, S.; Majid, A. A.; Lucero, J. M.; Crawford, J. M.; Carreon, M. A.; Koh, C. A. Metal−Organic Framework HKUST-1 Promotes Methane Hydrate Formation for Improved Gas Storage Capacity. *ACS Appl. Mater. Interfaces* **2020**, *12*, 53510−53518.
(21) Kim, N.-J.; Park, S.-S.; Shin, S.-W.; Hyun, J.-H.; Chun, W. An Experimental Investigation into the Effects of Zeolites on the Formation of Methane Hydrates. *Int. J. Energy Res.* **2015**, *39* (1), 26−32.
(22) Liu, H.; Zhan, S.; Guo, P.; Fan, S.; Zhang, S. Understanding the Characteristic of Methane Hydrate Equilibrium in Materials and Its Potential Application. *Chem. Eng. J.* **2018**, *349*, 775−781.
(23) Falconer, J. L.; Carreon, M. A.; Li, S.; Noble, R. D. Synthesis of Zeolites and Zeolite Membranes Using Multiple Structure Directing Agents. US No. 8302782B2, 2012.
(24) Poshusta, J. C.; Noble, R. D.; Falconer, J. L. Characterization of SAPO-34 Membranes by Water Adsorption. *J. Membr. Sci.* **2001**, *186* (1), 25−40.
(25) Kosinov, N.; Auffret, C.; Borghuis, G. J.; Sripathi, V. G. P.; Hensen, E. J. M. Influence of the Si/Al Ratio on the Separation Properties of SSZ-13 Zeolite Membranes. *J. Membr. Sci.* **2015**, *484*, 140−145.
(26) Nguyen, N. N.; Galib, M.; Nguyen, A. V. Critical Review on Gas Hydrate Formation at Solid Surfaces and in Confined Spaces - Why and How Does Interfacial Regime Matter? *Energy Fuels* **2020**, *34* (6), 6751−6760.
(27) Luo, Y.; Funke, H. H.; Falconer, J. L.; Noble, R. D. Adsorption of CO_2, CH_4, C_3H_8, and H_2O in SSZ-13, SAPO-34, and T-Type Zeolites. *Ind. Eng. Chem. Res.* **2016**, *55* (36), 9749−9757.
(28) Kim, D.; Ahn, Y. H.; Lee, H. Phase Equilibria of CO2 and CH4 Hydrates in Intergranular Meso/Macro Pores of MIL-53 Metal Organic Framework. *J. Chem. Eng. Data* **2015**, *60* (7), 2178−2185.
(29) Deimund, M. A.; Harrison, L.; Lunn, J. D.; Liu, Y.; Malek, A.; Shayib, R.; Davis, M. E. Effect of Heteroatom Concentration in SSZ-13 on the Methanol-to-Olefins Reaction. *ACS Catal.* **2016**, *6* (2), 542−550.

https://doi.org/10.1021/acsaem.1c02902
ACS Appl. Energy Mater. 2021, 4, 13420−13424